



HAL
open science

Subchondral tibial bone texture analysis predicts knee osteoarthritis progression: data from the Osteoarthritis Initiative

Thomas Janvier, Rachid Jennane, A. Valery, K. Harrar, M. Delplanque, C. Lelong,
D. Loeuille, Hechmi Toumi, Eric Lespessailles

► To cite this version:

Thomas Janvier, Rachid Jennane, A. Valery, K. Harrar, M. Delplanque, et al.. Subchondral tibial bone texture analysis predicts knee osteoarthritis progression: data from the Osteoarthritis Initiative. *Osteoarthritis and Cartilage*, 2017, 25 (2), pp.259-266. <10.1016/j.joca.2016.10.005>. <hal-01716368>

HAL Id: hal-01716368

<https://hal.science/hal-01716368v1>

Submitted on 25 Feb 2019

HAL is a multi-disciplinary open access archive for the deposit and dissemination of scientific research documents, whether they are published or not. The documents may come from teaching and research institutions in France or abroad, or from public or private research centers.

L'archive ouverte pluridisciplinaire **HAL**, est destinée au dépôt et à la diffusion de documents scientifiques de niveau recherche, publiés ou non, émanant des établissements d'enseignement et de recherche français ou étrangers, des laboratoires publics ou privés.



HAL Authorization

Accepted Manuscript

Subchondral tibial bone texture analysis predicts knee osteoarthritis progression: data from the Osteoarthritis Initiative

T. Janvier, R. Jennane, A. Valery, K. Harrar, M. Delplanque, C. Lelong, D. Loeuille, H. Toumi, E. Lespessailles, MD, PhD



PII: S1063-4584(16)30314-4

DOI: [10.1016/j.joca.2016.10.005](https://doi.org/10.1016/j.joca.2016.10.005)

Reference: YJOCA 3862

To appear in: *Osteoarthritis and Cartilage*

Received Date: 11 April 2016

Revised Date: 21 September 2016

Accepted Date: 5 October 2016

Please cite this article as: Janvier T, Jennane R, Valery A, Harrar K, Delplanque M, Lelong C, Loeuille D, Toumi H, Lespessailles E, Subchondral tibial bone texture analysis predicts knee osteoarthritis progression: data from the Osteoarthritis Initiative, *Osteoarthritis and Cartilage* (2016), doi: [10.1016/j.joca.2016.10.005](https://doi.org/10.1016/j.joca.2016.10.005).

This is a PDF file of an unedited manuscript that has been accepted for publication. As a service to our customers we are providing this early version of the manuscript. The manuscript will undergo copyediting, typesetting, and review of the resulting proof before it is published in its final form. Please note that during the production process errors may be discovered which could affect the content, and all legal disclaimers that apply to the journal pertain.

*Subchondral tibial bone texture analysis predicts knee osteoarthritis**progression: data from the Osteoarthritis Initiative**[Tibial bone texture & knee OA progression]*

T. Janvier^a, R. Jennane^a, A. Valery^b, K. Harrar^c, M. Delplanque^d, C. Lelong^e, D. Loeuille^f, H. Toumi^{a,b}, E. Lespessailles^{a,b*}

^a Univ. Orléans, I3MTO Laboratory, EA 4708, 45067 Orléans, France

^b CHR Orléans, Service de Rhumatologie, 45032 Orléans, France

^c Univ. M'Hamed Bougara Boumerdes, 35000 Boumerdes, Algeria

^d EOS imaging SA, 75011 Paris, France

^e Med-Imaps SASU, 337700 Mérignac, France

^f UMR 7561 – CHRU Nancy, 54511 Vandoeuvre les Nancy, France

* Corresponding author. Eric Lespessailles

MD, PhD

Regional Hospital of Orleans, 14 avenue de l'hôpital, 45067 Orleans Cedex 2

University of Orleans, I3MTO Laboratory, EA 4708, 45067 Orleans, France

Office: +33(0)238613151

E-mail : eric.lespessailles@chr-orleans.fr

Abstract

Objectives: To examine whether trabecular bone texture (TBT) parameters assessed on computed radiographs could predict knee osteoarthritis (OA) progression.

Methods: This study was performed using data from the Osteoarthritis Initiative. 1647 knees in 1124 patients had bilateral fixed flexion radiographs acquired 48 months apart. Images were semi-automatically segmented to extract a patchwork of regions of interest (ROI). A fractal texture analysis was performed using different methods. OA progression was defined as an increase in the joint space narrowing (JSN) over 48 months. The predictive ability of TBT was evaluated using logistic regression and receiver operating characteristic (ROC) curve. An optimization method for features selection was used to reduce the size of models and assess the impact of each ROI.

Results: Fractal dimensions were predictive of the JSN progression for each method tested with an area under the ROC curve (AUC) up to 0.71. Baseline JSN grade was not correlated with TBT parameters ($R < 0.21$) but had the same predictive capacity (AUC 0.71). The most predictive model included the clinical covariates (age, gender, body mass index), JSN and TBT parameters (AUC 0.77). From a statistical point of view we found higher differences in TBT parameters computed in medial ROI between progressors and non-progressors. However, the integration of TBT results from the whole patchwork including the lateral ROIs in the model provided the best predictive model.

Conclusions: Our findings indicate that TBT parameters assessed in different locations in the joint provided a good predictive ability to detect knee OA progression.

Keywords: fractal analysis, trabecular bone texture, knee osteoarthritis, subchondral bone, radiography

ACCEPTED MANUSCRIPT

1 Introduction

2 Osteoarthritis (OA) is the most common form of arthritis and is now considered as a
3 disease of the whole joint organ involving mainly the articular cartilage, subchondral bone
4 and synovial membrane but also the menisci and ligaments ¹. Recent research developments
5 in imaging options for OA showed that most of the studies in OA imaging focused on the
6 knee ^{2,3}. Conventional radiography is the currently accepted standard for monitoring OA
7 progression and the progressive loss of cartilage can be assessed by the reduction in the joint
8 space width (JSW) of the medial tibiofemoral compartment ⁴. JSW narrowing is considered as
9 a valid surrogate for the thickness of the articular cartilage, the meniscal loss and extrusion,
10 and is still the only imaging marker recommended by the Food and Drug Administration for
11 structural disease progression in clinical trials ⁵. There is some debate about the most relevant
12 definition of radiographic progression ^{6,7} and more recently on the inadequacy of conventional
13 radiography either for assessing eligibility purposes but also as an end point in OA disease-
14 modifying OA drugs trials ⁸.

15 It has been underlined that the identification of particular phenotypes of OA including
16 different profiles according to bone mineral density may lead to a better management of the
17 patient ^{6,9}. In line with these findings a renewed interest for the characterization of the
18 subchondral bone texture on X-ray radiographs has been developed ¹⁰. Several ways of
19 describing subchondral trabecular bone texture (TBT) roughness have been used such as
20 dissimilarity ^{11,12}, fractal dimension (FD) ^{13,14} or fractal signature (FS) ¹⁵⁻¹⁷. Fractal analysis
21 for the trabecular bone characterization of OA joints was introduced in the 1990's by Lynch et
22 al. ^{16,18}. It is a popular method due to its robustness against common radiographic problems
23 such as exposure or pixel size variations ¹⁸.

24 Previous work used subchondral TBT parameters to predict the knee OA progression
25 ^{12,15,19} and more recently the incident radiographic OA²⁰. However, most of them used small
26 samples of knee OA patients from a single clinical site of investigations. Consequently, herein
27 aim was to confirm the capacity of TBT parameters to discriminate patients with or without
28 knee OA progression and to predict this progression using data from a large, multicenter and
29 open access database. We also focused on the assessment of the best descriptors for TBT
30 characterization and on the choice of the region of interest (ROI) in the subchondral bone.

31 **Material & Methods**

32 Patients

33 Data used in the preparation of this article were obtained from the Osteoarthritis Initiative
34 (OAI) database ²¹, which is available for public access at <http://www.oai.ucsf.edu/>. This
35 database contains bilateral fixed flexion knee radiographs of 4796 patients followed since
36 2008. It is a multi-center and multi-equipment study. To avoid any digitalization artifacts,
37 only the computed radiographs (CR), identified from the DICOM headers, were considered.
38 In order to separate the different populations, only the knees from patients for whom the
39 assessment of Kellgren-Lawrence (KL) ²² and Osteoarthritis Research Society International
40 (OARSI) ²³ grades as well as their clinical covariates: age, gender and body mass index (BMI)
41 were available online, have been included. From this subset, the knees with preexisting non-
42 severe OA at baseline were included in this study (preexisting non-severe OA was defined by
43 a KL grade $\in [2; 4[$ in order to focus on the non-doubtfully OA patients with a worsening
44 potential). Radiographs that presented knees with material, misalignment, radiographic
45 defects or poor quality as defined in ²⁴ were removed during the segmentation process.

46 Finally, the subpopulation used in this work consisted of 1124 patients (624 women and
47 500 men) in whom 1647 knees were radiographed and graded for both KL and OARSI scales.
48 Table 1 provides the characteristics of the subgroup used in the present study. Established
49 radiographic tibiofemoral OA cases and controls were selected as shown in Figure 1.

50 Acquisition and grading

51 During 72 months, participants had annual bilateral posteroanterior fixed flexion knee
52 radiographs using the fixed flexion standardized positioner SynaFlexer²⁵. In the present
53 study, only the baseline radiographs were used. Radiographs were provided as 16-bits
54 DICOM files from which we extracted parameters such as the date of acquisition, the
55 modality or the pixel spacing. The resolution was not standardized in the database, the pixel
56 size was variable from 150 to 200 μm for CR. Details concerning the acquisition²⁴ and
57 grading²⁶ protocols in the OAI study are available online.

58 OA grouping

59 In this population, patients with or without OA progression were selected using the
60 following definition: OA progressors (cases) designate patients with an increased medial JSN
61 grade over the 48 months; while OA non-progressors (controls) designate patients with a
62 constant medial JSN grade from baseline to 48 months acquisition. Table 1 provides the
63 demographic data and OARSI grades for the two subgroups identified.

64 Regions of interest

65 A semi-automatic method was used to extract the trabecular bone ROIs. This method
66 computes a patchwork of 16 square ROIs mapping the whole joint trabecular area. First, a
67 trained operator (T.J) marked the tibial spines and the lateral and medial extremities of the

68 tibia. Second, the algorithm approximated the tibial subchondral bone plate as the brightest
69 path going through these anatomical markers. Third, this estimation was used to fit the tibial
70 plate orientation and clamp our patchwork under the cortical plates. To avoid subchondral
71 bone sclerosis, a vertical adjustment of the ROI position was performed as proposed in ¹³. To
72 prevent periarticular osteophytes and fibular head overlay, an offset equal to 10% of the knee
73 width was applied to the horizontal positioning. The ROIs dimensions were proportional to
74 the knee width defined as the distance between the outer tibial margins. This provided an
75 average side length of 62 ± 7 pixels, which represents a square of 1 ± 0.1 cm side. Figure 2
76 illustrates the result of the mapping using a 4-by-7 square patchwork.

77 Texture analysis

78 Fractal analysis is a suitable method for radiographic texture analysis since its parameters
79 are linked to the 3D microarchitecture of the trabecular bone as shown at the calcaneus and
80 vertebrae ²⁷⁻³⁰. It is also considered as robust to radiographic magnification and projection
81 ^{18,31}, and inhomogeneous contrast ^{18,27}. Many methods have been developed to compute the
82 FD of a signal ³²⁻³⁵. In this study we compared three methods used for the trabecular bone
83 characterization, the common technique of the fractal signature analysis (FSA) ¹⁸, the Whittle
84 estimator (WhE) ^{35,36} and a method based on the quadratic variations (VAR) ³⁴ used in DXA
85 imaging ³⁷. In the following we will use the H parameter, which is directly linked to the FD
86 and the roughness of the signal. Each method is described briefly below; further details are
87 presented in supplementary files:

88

89 **FSA estimator (FSA)** ¹⁸ is the most common technique to compute the FD particularly in
90 OA research field. The principle is to dilate and erode the signal using different sizes of
91 structuring elements (SE) and compute the log-ratio of the area between the dilated / eroded

92 signals, and the size of the structuring element. In other words, FSA computes the differences
93 between an under and over estimation of the signal according to the scale of observation and
94 extract the fractal dimension (which is linked to the roughness) from the log-log plot
95 regression of the curve. In this work, we used a line shape SE (which size varies from 3 pixels
96 to half the length of the ROI) to compute the H in different directions. The fractal parameter
97 H was computed as the slope of the log-log curve.

98 **Quadratic variations estimator (VAR)** ³⁸ is a roughness measurement based on the
99 variations of the pixels intensity for a defined step. Similarly to the FSA method, H can be
100 computed from the slope of the log-curve of the quadratic variations against the scale. In this
101 work we used the approach of Istaş & Lang ³⁴, computing H as the slope at the origin.

102 **Whittle estimator (WhE)** ³⁶ is a maximum likelihood estimator based on the
103 approximation of the likelihood function of a fractal signal increments. The aim is to fit the
104 characterized texture to a fractal model driven by a single parameter H. This estimator is the
105 most accurate in term of bias and variance when applied to synthetic fractal images ^{36,39}.

106

107 **Anisotropy:** As shown in ^{12,19}, the tibial trabecular bone is an anisotropic material. To
108 consider the anisotropy into our descriptors, each analysis was performed on each ROI in
109 different directions $\theta = \{0^\circ; 45^\circ; 90^\circ; 135^\circ\}$ providing exact computation of the roughness
110 parameters without any interpolation. The retained values used are the H parameters obtained
111 for 0° and 90° orientations (H_0, H_{90}) and the averaged value (H_{mean}) for $H_{\theta=\{0^\circ;45^\circ;90^\circ;135^\circ\}}$.

112

113 Each method was implemented in C++/MATLAB and validated on synthetic fractal
114 images before processing the TBT ROIs.

115 Statistical analysis

116 First, the clinical covariates were investigated using the non-parametric test of Mann-
 117 Whitney for the numerical data and the Chi-square test for the nominal data. Using the
 118 obtained values (Table 1), we adjusted the results for the TBT parameters (Figure 3) using an
 119 ANCOVA with the following linear model: $\text{Group} \sim \text{TBT} + \text{Gender} + \text{BMI}$. The
 120 associations between clinical covariates, KL and OARSI grades and TBT parameters were
 121 evaluated using Pearson's correlation for the age and the BMI and Spearman's correlation for
 122 the KL and medial JSN grades at baseline.

123 Second, the prediction was evaluated using a logistic regression with several models
 124 including the clinical covariates, the center, the medial JSN grade at baseline and the different
 125 TBT parameters – H_0, H_{90}, H_{mean} computed with the different methods – WhE, FSA, Var . A
 126 total of six models were trained:

- 127 1. Clinical covariates i.e: Age + Gender + BMI + Center
- 128 2. TBT using WhE + clinical covariates i.e: WhE + Age + Gender + BMI + Center
- 129 3. TBT using FSA + clinical covariates i.e: FSA + Age + Gender + BMI + Center
- 130 4. TBT using VAR + clinical covariates i.e: VAR + Age + Gender + BMI + Center
- 131 5. JSN grade + clinical covariates i.e: JSN + Age + Gender + BMI + Center
- 132 6. TBT using WhE + JSN grade + clinical covariates i.e: WhE + JSN + Age + Gender
 133 + BMI + Center

134 As there are 3 TBT parameters computed in 16 ROIs, this results in 48 descriptors for each
 135 method (WhE, FSA, Var). In order to evaluate the effect of such large models on the
 136 prediction results, we trained the different models in three different ways, all avoiding
 137 interactions between the variables:

- 138 • **Complete:** the models were evaluated including the 48 TBT descriptors

- 139 • **Partial:** TBT parameters were restricted to H_{90} in the subchondral strip (7 upper
140 ROIs in Figure 2) leading to 7 TBT descriptors in order to show the role of the
141 ‘most significantly affected part of the bone’.
- 142 • **Optimized:** a backward selection of the variables in the full models was
143 automatically performed using the Akaike Information Criterion (AIC) as iterative
144 criteria, resulting in 7, 10 and 15 TBT markers for WhE, VAR and FSA methods
145 respectively. This AIC penalizes the complex models limiting the overfitting. The
146 algorithm evaluates the AIC when removing iteratively each parameter and
147 preserves the most efficient model.

148 For each model/method a 10-fold cross-validation was repeated 300 times to build the
149 receiver operating characteristic (ROC) curves. The area under the curve (AUC) was used as a
150 performance criterion. The comparison between the models was based on the ROC curves
151 using the DeLong method⁴⁰.

152 All statistical analyses were performed using R (<https://www.r-project.org>) and the
153 packages MASS (for the stepwise AIC optimization), Caret (for the cross-validation training)
154 and pROC (for ROC curves and comparisons). Documentation for these packages is available
155 online at <https://cran.r-project.org/web/packages/>.

156 **Results**

157 Clinical covariates

158 The clinical covariates are presented in Table 1 where the *p-values* indicate the
159 significance level of the separation between progressors and non-progressors for each
160 parameter at baseline. First, it can be noticed that dependencies exist between the gender (P
161 < 0.001) and BMI ($P = 0.002$) of the patients and the progression of their OA. No significant
162 differences were found between ages in the two groups ($P = 0.9$). Although the OAI database

163 is multi-centric and multi-equipment, no significant center effect was observed on OA
164 progression ($P = 0.5$). Baseline medial JSN grade was significantly different in the two groups
165 ($P < 0.001$).

166 Texture Parameters

167 Figure 3 presents the *p-values* for each TBT descriptor adjusted for gender and BMI.
168 Results differed according to ROIs and to the fractal analysis method.

169 **Horizontal FD (0°)** was not significantly different between progressors and non-progressors
170 except for the FSA method in the medial extremities of the patchwork (see Figure 3).

171 **Vertical FD (90°)** was significantly higher in progressors compared to non-progressors in
172 almost every medial ROI for the three methods tested. However, results were more consistent
173 along the whole patchwork for the WhE method with a decreasing gradient from subchondral
174 medial area to the lateral deeper trabecular bone (Figure 3). The VAR method provided
175 almost the same results as the WhE with lower significant *p-values*. FSA was more
176 discriminant between progressors and non progressors in the lower part of the patchwork.

177 **Average FD (360°)** analyses as illustrated in Figure 3, did not add much to the 90° and 0°
178 results.

179 Associations of TBT parameters and patient characteristics

180 The correlations between the TBT parameters and the subjects characteristics were
181 computed separately for all TBT parameters applied on each ROI. No significant correlations
182 were found at baseline between TBT parameters and clinical covariates nor OARSI grades.
183 The maximum value for the correlation coefficient R was found for the association between
184 TBT and the gender with $R -0.34$ ($-0.38 -0.30$) 95% confidence interval (CI). Targeting the
185 JSN, R ranged from 0 ($-0.05 0.05$) 95% CI to -0.21 ($-0.25 -0.16$) 95% CI.

186 OA progression prediction

187 Figure 4, Figure 5 and Figure 6 present the performances of the models tested.

188 **Complete models** including every couple (TBT-descriptor, ROI) showed similar results for
189 each fractal analysis method (models 2, 3 and 4 are statistically not different from each other:
190 $P > 0.5$). Each method provided significantly similar results to the model using the JSN grade
191 (models 2, 3 and 4 are statistically similar to model 5: $P > 0.5$). The combination of TBT
192 parameters and the medial JSN grade in model 6 provided the best predictive model with an
193 AUC of 0.76 which is significantly different from the other models (models 1, 2, 3, 4 and 5
194 were all statistically different from model 6: $P < 0.001$).

195 **Partial models** showed different results than the complete ones. The FSA model was no
196 longer equal to the WhE and VAR models (models 2 and 4 are statistically different from
197 model 3: $P < 0.001$) and can be assimilated to the model with only the clinical covariates
198 (model 3 is not statistically different from model 1: $P > 0.1$). The best predictive model
199 remained model 6 with an AUC of 0.73, still significantly higher than the other models
200 ($P < 0.001$).

201 **AIC optimized models** provided the same results as the complete ones for the individual
202 models 2, 3, 4 and 5, blurring the differences between the fractal analysis methods.
203 Differences between models 2, 3 and 4 were improved but not significantly ($P > 0.3$). Model
204 6 remained the best model with an AUC of 0.74 and a significant difference compared to the
205 other models ($P < 0.001$).

206 Discussion

207 In the present study, we have shown in the large sample of the OAI database that tibial
208 TBT fractal parameters were predictive of the JSN in the medial compartment over 48 months

209 in patients with prevalent OA. The three different fractal analysis methods (WhE, FSA and
210 VAR) provided consistent results in their capacity to predict OA progression. In line with our
211 data, previous works have already highlighted the interest of the TBT parameters to separate
212 OA progressors from non progressors^{12,15,19}.

213 Messent et al.¹⁹ assessed over 24 months the changes in the subchondral and subarticular
214 trabecular bone for 40 patients with medial compartment knee OA at baseline. They tested the
215 ability of the FSA method to distinguish between the progressors and non-progressors over 48
216 months. They found longitudinal FD decreases in both vertical and horizontal directions in all
217 OA knees. This decrease was significantly greater in patients with JSN > 0.2mm/year.

218 Compared to the Messent, Kraus et al.¹⁵ added clinical covariates to the TBT parameters in
219 order to build predictive models of OA progression. Over a larger dataset (138-vs-40
220 patients) and for a longer period (3-vs-2 years) they showed that the better model for this task
221 included a combination of FSA, knee alignment and clinical covariates (AUC 0.79).

222 More recently, Woloszynski et al.¹² have investigated the ability of TBT parameters to
223 predict OA progression over a 4-year period. The analysis was conducted on 105 subjects in
224 whom longitudinal digitized knee radiographs were obtained. They have found that the
225 highest prediction accuracy (AUC 0.77) was provided by a model including textural
226 parameters from a medial subchondral ROI with adjustment for age, BMI and gender. They
227 used different descriptors for the roughness, based on the Gaussian kernels decomposition and
228 focused on the anisotropic property of the subchondral knee TBT.

229 Effect of the fractal analysis method

230 The consistency of our results for the prediction of OA using the three different fractal
231 analysis methods (WhE, FSA and VAR) indicates that the employed algorithm might have a
232 low effect on the prediction results. It would also explain the consistency between the results

233 of Woloszynski¹² and Kraus¹⁵ who computed roughness parameters using two different
234 methods. However, when focusing on the individual ROIs the methods tested in this work
235 provided different discriminant values in the patchwork (in Figure 3). This result shows
236 differences in terms of sensitivity between the approach and could be explained by the fact
237 that the three methods (WhE, FSA and VAR) were applied to non-exact fractal textures as
238 suggested by the findings in the calcaneus TBT³⁵.

239 Effect of the ROI selection

240 Although previous studies^{12,15,19} have used a reduced number of fixed ROIs, we used a
241 patchwork that covers the full proximal tibial bone inspired by^{11,41}. The subchondral medial
242 area provided more relevant ROIs to focus on. However, the lateral area provided some
243 significant differences for both WhE and FSA approaches. The absence of statistically
244 significant differences in the lateral ROIs should not be claimed to ignore this area of the
245 bone. Furthermore, the automated pruning of predictive models confirmed that the lateral side
246 also contains information that, despite their lower significant value for discrimination,
247 improved the prediction (see red ROIs in Figure 3). The same conclusions can be drawn for
248 the deeper layers of ROIs and not only those ROIs immediately above the subchondral bone
249 plate. Past studies focused on the subchondral part of the bone ignoring deeper areas,
250 however, WhE and FSA highlighted ROIs with significant differences up to 3 cm under the
251 tibial plate.

252 These aforementioned observations may lead to the hypothesis that the remodeling
253 process involved in the progression of OA is not limited in specific subregions of interest of
254 either medial or lateral tibial subchondral bone areas. It would also implicated both
255 subchondral cortical bone and subchondral trabecular bone located in deeper areas that might

256 intervene in the complex interactions and cross talks between cartilage and bone tissue in the
257 model of knee OA progression.

258 Effect of the orientation

259 We used only the two main directions (horizontal and vertical) plus an average of the
260 parameter computed every 45°. The estimation of the parameters along the two main loading
261 axes in Figure 3 allowed us to show and confirm that the main changes appear in the vertical
262 (compression) direction. The FD in OA progressors was higher along the vertical direction
263 and lower in the horizontal compared to the control group.

264 As suggested in ¹⁵, our findings show that the increase of the roughness in the compression
265 orientation in progressors reflects an increased complexity in the vertical trabeculae
266 organization, such as a higher trabecular number and a higher gap between coarser trabeculae
267 reflecting an erratic bone remodeling process. Conversely, the decrease in the horizontal FD
268 in progressors and consequently the smoothing of the texture could be explained by a
269 coarsening of the trabeculae.

270 Comparison to the JSN grade

271 Our findings demonstrated that the TBT parameters could predict knee OA progression
272 with the same predictive capacity as the initial JSN grade. In our study, the baseline JSN
273 grade was not correlated with the TBT parameters whatever the ROI, the algorithm or the
274 orientation considered. This would indicate that TBT parameters and JSN capture different
275 information about the global joint degradation status. This was further confirmed with the
276 improvement of the AUC when using both TBT and JSN in the same model and by the
277 stepwise optimization of the complete model that kept both the initial medial JSN grade and
278 several TBT parameters. This result differs with Woloszynski ¹² and Kraus ¹⁵ observations

279 where the initial JSN grade was not predictive of OA progression. The lack of the predictive
280 value of baseline JSN in their studies might be explained by the proportion of the JSN grades
281 at baseline as for both studies they included more patients with lower JSN grades (merely
282 90% of JSN < 2 in Woloszynski work's ¹⁷, and inclusion of KL = 1 with consequently lower
283 JSN grades in Kraus works ¹⁵). We could hypothesis that TBT parameters would be better
284 indicators for early OA stages prediction while JSN would be a better marker of late OA
285 progression stage.

286 Limitations and strengths

287 First, the JSN score used was only a discrete ordinal grade and it might be more accurate to
288 use the continuous value of the JSW to check if the prediction of OA progression can be
289 improved.

290 Second, the OA progression was defined as an increase of the medial JSN grade. This
291 definition was used to compare our results to the aforementioned studies ^{12,15,19}. It should
292 therefore be interesting to examine if the influence of the initial grade of JSN and the speed of
293 narrowing could be predicted by TBT parameters changes. It has been found by Woloszynski
294 et al that late OA progression prediction by TBT analysis might be more accurate than early
295 stages of OA progression ¹².

296 Third, we only considered for analysis the set of digital radiographs. In the OAI study, due to
297 the multicenter and multi-equipment nature of the study some patients had conventional
298 radiographs digitized for a second time. Moreover, we performed a retrospective analysis of
299 knee OA progression in the OAI database thus not including potential confounders that could
300 only be controlled in a prospective study.

301 Our study has several important strengths. We used the large OAI database (more than
302 1000 patients) of knee images and assessed the potential of different TBT analyses for the

303 prediction of OA progression. In addition in this database, the X-ray devices had not been x-
304 calibrated, neither the variations in the acquisition parameters had been taken into account nor
305 the impact of the soft tissue in the x-ray absorption and diffusion. This can appear as a
306 limitation, however, our models managed to predict the knee OA progression. To insure that
307 the results were not the consequences of a center effect we investigated the associations
308 between the centers and the progression. The lack of center effect underlines the robustness of
309 our approach since we were able to predict knee OA progression whatever the center. We also
310 adjusted for potential clinical risk factors for OA progression (e.g. age, gender, BMI and JSN
311 grade) in order to identify risk factors for various patterns of knee OA progression over time.
312 In addition, due to our cross validation statistical approach we were able to build conservative
313 estimates in our predictive models

314 Summary

315 In summary, over 4 years of follow up our findings suggest that in addition to baseline JSN
316 grade, TBT parameters predict knee OA progression on digital radiographs. TBT parameters
317 analyses might contribute to monitor the OA progression. Furthermore it could be relevant to
318 select subgroup of knee OA patients that might be enrolled in clinical trials aiming at the
319 evaluation of potentially costly drugs (biotherapies) that target the progression of the disease.

320 **Acknowledgments**

321 The authors would like to thank the OAI study participants and clinic staff as well as the
322 coordinating center at UCSF. The authors wish to thank the ANR for the financial support
323 under the project ANR-12-TECS-0016-01. We acknowledge Mrs Villequenault for type
324 writing the manuscript.

325

326 **Author Contributions**

327 All authors contributed to the conception and design of the study, analysis and
328 interpretation of data, drafting the article and revising it critically for important intellectual
329 content, and approved the final version submitted. Dr Lespessailles takes responsibility for the
330 integrity of the work as a whole, from inception to finished article.

331 **Role of the funding sources**

332 Thomas Janvier (PhD student) was funded by ANR-12-TECS-0016-01.

333 Funding sources had no role in the study design, collection, analysis and interpretation of
334 the data or the decision to submit the manuscript for publication.

335 **Conflict of interest**

336 All authors state that they have no conflicts of interest.

337 **References**

338

- 339 1. Loeser RF, Goldring SR, Scanzello CR, Goldring MB. Osteoarthritis: A disease of the
340 joint as an organ. *Arthritis Rheum.* 2012;64(6):1697-1707. doi:10.1002/art.34453.
- 341 2. Guermazi A, Roemer FW, Felson DT, Brandt KD. Unresolved questions in
342 rheumatology: Motion for debate: Osteoarthritis clinical trials have not identified
343 efficacious therapies because traditional imaging outcome measures are inadequate.
344 *Arthritis Rheum.* 2013;65(11):2748-2758. doi:10.1002/art.38086.
- 345 3. Eckstein F, Kwok CK, Link TM. Imaging research results from the Osteoarthritis
346 Initiative (OAI): a review and lessons learned 10 years after start of enrolment. *Ann*
347 *Rheum Dis.* 2014;2006(Figure 3):1289-1300. doi:10.1136/annrheumdis-2014-205310.
- 348 4. Felson DT, Niu J, Guermazi A, Sack B, Aliabadi P. Defining radiographic incidence
349 and progression of knee osteoarthritis: suggested modifications of the Kellgren and

- 350 Lawrence scale. *Ann Rheum Dis.* 2011;70(11):1884-1886.
351 doi:10.1136/ard.2011.155119.
- 352 5. Buckland-wright C. Which radiographic techniques should we use for research and
353 clinical practice? *Best Pract Res Clin Rheumatol.* 2006;20(1):39-55.
354 doi:10.1016/j.berh.2005.08.002.
- 355 6. Arden N, Richette P, Cooper C, et al. Can We Identify Patients with High Risk of
356 Osteoarthritis Progression Who Will Respond to Treatment? A Focus on Biomarkers
357 and Frailty. *Drugs Aging.* 2015;32(7):525-535. doi:10.1007/s40266-015-0276-7.
- 358 7. LaValley MP, McAlindon TE, Chaisson CE, Levy D, Felson DT. The validity of
359 different definitions of radiographic worsening for longitudinal studies of knee
360 osteoarthritis. *J Clin Epidemiol.* 2001;54(1):30-39. doi:10.1016/S0895-4356(00)00273-
361 0.
- 362 8. Lories RJ, Luyten FP. the Bone–Cartilage Unit in Osteoarthritis. *Nat Publ Gr.*
363 2010;7(10):43-49. doi:10.1038/nrrheum.2010.197.
- 364 9. Kinds MB, Marijnissen ACA, Viergever MA, Emans PJ, Lafeber FPJG, Welsing PMJ.
365 Identifying Phenotypes of Knee Osteoarthritis by Separate Quantitative Radiographic
366 Features May Improve Patient Selection for More Targeted Treatment. *J Rheumatol.*
367 2013;40(6):891-902. doi:10.3899/jrheum.121004.
- 368 10. Lespessailles E, Jennane R. Assessment of bone mineral density and radiographic
369 texture analysis at the tibial subchondral bone. *Osteoporos Int.* 2012;23(8):871-876.
370 doi:10.1007/s00198-012-2167-7.
- 371 11. Woloszynski T, Podsiadlo P, Stachowiak GW, Kurzynski M. A signature dissimilarity
372 measure for trabecular bone texture in knee radiographs. *Med Phys.* 2010;37(5):2030-
373 2042. doi:Doi 10.1118/1.3373522.
- 374 12. Woloszynski T, Podsiadlo P, Stachowiak GW, Kurzynski M, Lohmander LS, Englund
375 M. Prediction of progression of radiographic knee osteoarthritis using tibial trabecular
376 bone texture. *Arthritis Rheum.* 2012;64(3):688-695. doi:10.1002/art.33410.
- 377 13. Podsiadlo P, Wolski M, Stachowiak GW. Automated selection of trabecular bone
378 regions in knee radiographs. *Med Phys.* 2008;35(September 2007):1870-1883.
379 doi:10.1118/1.2905025.
- 380 14. Podsiadlo P, Cicuttini FM, Wolski M, Stachowiak GW, Wluka AE. Trabecular bone
381 texture detected by plain radiography is associated with an increased risk of knee
382 replacement in patients with osteoarthritis: A 6 year prospective follow up study.
383 *Osteoarthr Cartil.* 2014;22(1):71-75. doi:10.1016/j.joca.2013.10.017.
- 384 15. Kraus VB, Feng S, Wang S, et al. Trabecular morphometry by fractal signature
385 analysis is a novel marker of osteoarthritis progression. *Arthritis Rheum.*

- 386 2009;60(12):3711-3722. doi:10.1002/art.25012.
- 387 16. Lynch JA, Hawkes DJ, Buckland-Wright JC. Analysis of texture in macroradiographs
388 of osteoarthritic knees, using the fractal signature. *Phys Med Biol.* 1991;36(6):709-722.
389 doi:10.1088/0031-9155/36/6/001.
- 390 17. Kraus VB, Feng S, Wang S, et al. Subchondral bone trabecular integrity predicts and
391 changes concurrently with radiographic and magnetic resonance imaging-determined
392 knee osteoarthritis progression. *Arthritis Rheum.* 2013;65(7):1812-1821.
393 doi:10.1002/art.37970.
- 394 18. Lynch JA, Hawkes DJ, Buckland-Wright JC. A robust and accurate method for
395 calculating the fractal signature of texture in macroradiographs of osteoarthritic knees.
396 *Med Informatics.* 1991;16(2):241-251. doi:10.3109/14639239109012130.
- 397 19. Messent E a, Ward RJ, Tonkin CJ, Buckland-Wright C. Tibial cancellous bone changes
398 in patients with knee osteoarthritis. A short-term longitudinal study using Fractal
399 Signature Analysis. *Osteoarthr Cartil.* 2005;13(6):463-470.
400 doi:10.1016/j.joca.2005.01.007.
- 401 20. Podsiadlo P, Nevitt MC, Wolski M, et al. Baseline trabecular bone and its relation to
402 incident radiographic knee osteoarthritis and increase in joint space narrowing score:
403 directional fractal signature analysis in the MOST study. *Osteoarthr Cartil.* May 2016.
404 doi:10.1016/j.joca.2016.05.003.
- 405 21. Nevitt M, Felson D, Lester G. *The Osteoarthritis Initiative: Protocol for the Cohort
406 Study.*; 2006.
- 407 22. Kellgren JH, Lawrence JS. Radiological Assessment of. *Ann Rheum Dis.*
408 1957;16(April 2009):494-502. doi:10.1136/ard.16.4.494.
- 409 23. Altman RD, Gold GE. Atlas of individual radiographic features in osteoarthritis,
410 revised. *Osteoarthr Cartil.* 2007;15(SUPPL. 1):A1-A56.
411 doi:10.1016/j.joca.2006.11.009.
- 412 24. Osteoarthritis Initiative. Radiographic Procedure Manual for Examinations of the Knee
413 , Hand , Pelvis and Lower Limbs. [http://oai.epi-
414 ucsf.org/datarelease/operationsmanuals/radiographicmanual.pdf](http://oai.epi-ucsf.org/datarelease/operationsmanuals/radiographicmanual.pdf). Published 2006.
- 415 25. Kothari M, Guermazi A, von Ingersleben G, et al. Fixed-flexion radiography of the
416 knee provides reproducible joint space width measurements in osteoarthritis. *Eur
417 Radiol.* 2004;14(9):1568-1573. doi:10.1007/s00330-004-2312-6.
- 418 26. Osteoarthritis Initiative. *Central Reading of Knee X-Rays for Kellgren & Lawrence
419 Grade and Individual Radiographic Features of Tibiofemoral Knee OA.*; 2016.
- 420 27. Pothuaud L, Benhamou CL, Porion P, Lespessailles E, Harba R, Levitz P. Fractal
421 Dimension of Trabecular Bone Projection Texture Is Related to Three-Dimensional

- 422 Microarchitecture. *J Bone Miner Res.* 2000;15(4):691-699.
423 doi:10.1359/jbmr.2000.15.4.691.
- 424 28. Jennane R, Harba R, Lemineur G, Bretteil S, Estrade A, Benhamou CL. Estimation of
425 the 3D self-similarity parameter of trabecular bone from its 2D projection. *Med Image*
426 *Anal.* 2007;11(1):91-98. doi:10.1016/j.media.2006.11.001.
- 427 29. Hans D, Barthe N, Boutroy S, Pothuaud L, Winzenrieth R, Krieg MA. Correlations
428 Between Trabecular Bone Score, Measured Using Anteroposterior Dual-Energy X-Ray
429 Absorptiometry Acquisition, and 3-Dimensional Parameters of Bone
430 Microarchitecture: An Experimental Study on Human Cadaver Vertebrae. *J Clin*
431 *Densitom.* 2011;14(3):302-312. doi:10.1016/j.jocd.2011.05.005.
- 432 30. Hirvasniemi J, Thevenot J, Kokkonen HT, et al. Correlation of Subchondral Bone
433 Density and Structure from Plain Radiographs with Micro Computed Tomography Ex
434 Vivo. *Ann Biomed Eng.* 2016;44(5):1698-1709. doi:10.1007/s10439-015-1452-y.
- 435 31. Winzenrieth R, Michelet F, Hans D. Three-Dimensional (3D) microarchitecture
436 correlations with 2d projection image gray-level variations assessed by trabecular bone
437 score using high-resolution computed tomographic acquisitions: Effects of resolution
438 and noise. *J Clin Densitom.* 2013;16(3):287-296. doi:10.1016/j.jocd.2012.05.001.
- 439 32. Podsiadlo P, Dahl L, Englund M, Lohmander LS, Stachowiak GW. Differences in
440 trabecular bone texture between knees with and without radiographic osteoarthritis
441 detected by fractal methods. *Osteoarthr Cartil.* 2008;16(3):323-329.
442 doi:10.1016/j.joca.2007.07.010.
- 443 33. Peleg S, Naor J, Hartley R, Avnir D. Multiple Resolution Texture Analysis and
444 Classification. *IEEE Trans Pattern Anal Mach Intell.* 1984;PAMI-6(4):518-523.
445 doi:10.1109/TPAMI.1984.4767557.
- 446 34. Istas J, Lang G. Quadratic variations and estimation of the local Holder index of a
447 Gaussian process. In: *Ann I H Poincare-Pr.* Vol 33. Elsevier; 1997:407-436.
- 448 35. Harrar K, Hamami L, Lespessailles E, Jennane R. Piecewise Whittle estimator for
449 trabecular bone radiograph characterization. *Biomed Signal Process Control.*
450 2013;8(6):657-666. doi:10.1016/j.bspc.2013.06.009.
- 451 36. Whittle P. Estimation and information in stationary time series. *Ark för Mat.*
452 1953;2(5):423-434. doi:10.1007/BF02590998.
- 453 37. Harvey NC, Glüer CC, Binkley N, et al. Trabecular bone score (TBS) as a new
454 complementary approach for osteoporosis evaluation in clinical practice. *Bone.*
455 2015;78:216-224. doi:10.1016/j.bone.2015.05.016.
- 456 38. Guyon X, Leon J. Convergence en loi des H-variations d'un processus gaussien
457 stationnaire sur R. *Ann l'IHP Probab Stat.* 1989;25(3):265-282.

- 458 39. Dahlhaus R. Efficient Parameter Estimation for Self-Similar Processes. *Ann Stat.*
459 1989;17(4):1749-1766. doi:10.1214/aos/1176347393.
- 460 40. DeLong ER, DeLong DM, Clarke-Pearson DL. Comparing the areas under two or more
461 correlated receiver operating characteristic curves: a nonparametric approach.
462 *Biometrics.* 1988;44(3):837-845. doi:10.2307/2531595.
- 463 41. Shamir L, Ling SM, Scott W, Hochberg M, Ferrucci L, Goldberg IG. Early detection of
464 radiographic knee osteoarthritis using computer-aided analysis. *Osteoarthr Cartil.*
465 2009;17(10):1307-1312. doi:10.1016/j.joca.2009.04.010.
- 466

467 Illustrations & legends

468 Figure 1: Flowchart diagram illustrating the selection of study subjects from the OAI dataset (n is the
469 number of patients and k the corresponding number of knee radiographs at baseline). From the OAI
470 initial database, non-severe OA patients ($2 \leq \text{KL} < 4$) with graded knees and baseline computed
471 radiographs were included.

472 Table 1: Characteristics of the 1124 patients - 1647 knee radiographs included in the study. Gender
473 and Center characteristics did not change for baseline and 48 month, p -values are the significance
474 levels of separation between progressors and controls for the different characteristics at baseline.

475 Figure 2: Knee trabecular bone mapping using a semi-automatic algorithm for ROIs selection. Dots
476 are the anatomical markers manually defined, the highlighted line is the estimated tibial edge and the
477 squared patchwork defines the ROIs.

478 Figure 3: Obtained p -values for TBT parameters in progressors versus controls. Values indicated in
479 each ROI are the p -values in scientific notation (i.e 5E-02 means 0.05), significant values are
480 highlighted. Red rectangles represent the ROIs automatically selected by the AIC-based models
481 optimization. The columns: WhE, FSA and VAR correspond to the different methods of analysis
482 while the lines: 0° , 90° and 360° correspond to the different directions of analysis (horizontal, vertical
483 and the mean value computed for each 45°).

484 Figure 4: ROC curves obtained for the OA progression prediction using a 10-folds cross validation
485 repeated 300 times. The complete models include Age, Gender, BMI and the 3 TBT descriptors
486 computed over all ROIs (48 TBT markers).

487 Figure 5: Obtained ROC curves for the OA progression prediction using a 10-folds cross validation
488 repeated 300 times. The partial models includes Age, Gender, BMI and the TBT vertical descriptor
489 computed over the 7 subchondral ROIs (7 TBT markers).

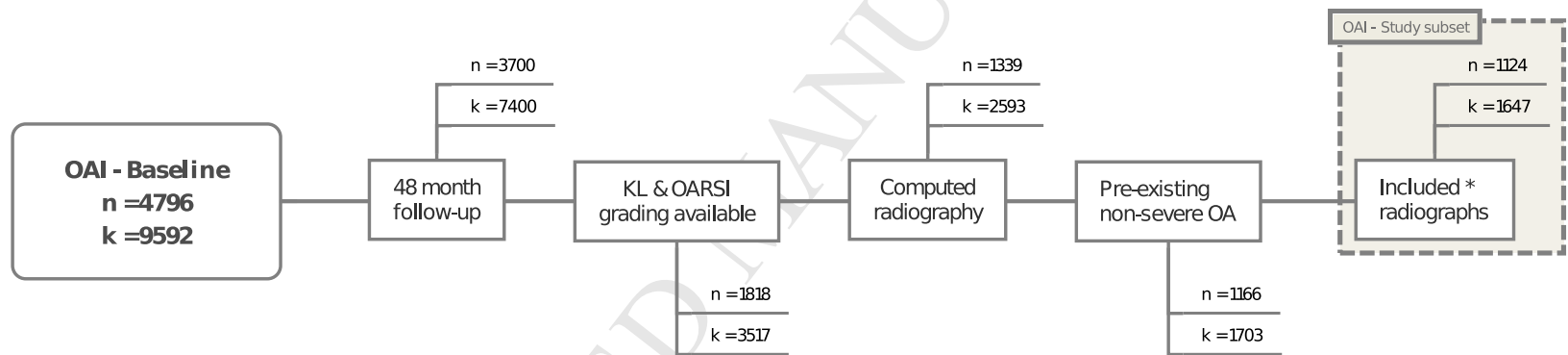
490 Figure 6: Obtained ROC curves for the OA progression prediction using a 10-folds cross validation
491 repeated 300 times. The optimized models were built from the complete models using a stepwise
492 backward selection minimizing the AUC.

ACCEPTED MANUSCRIPT

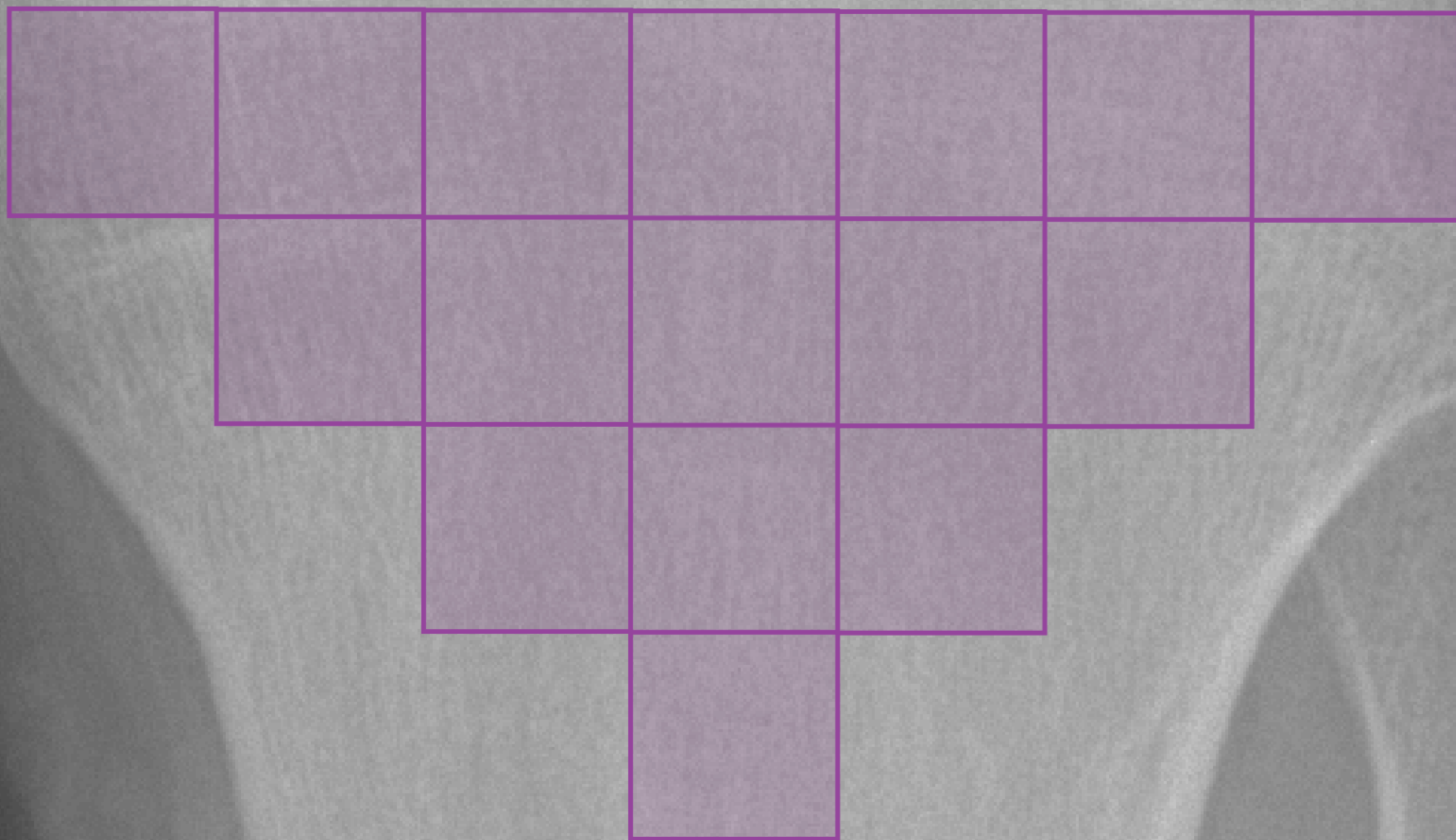
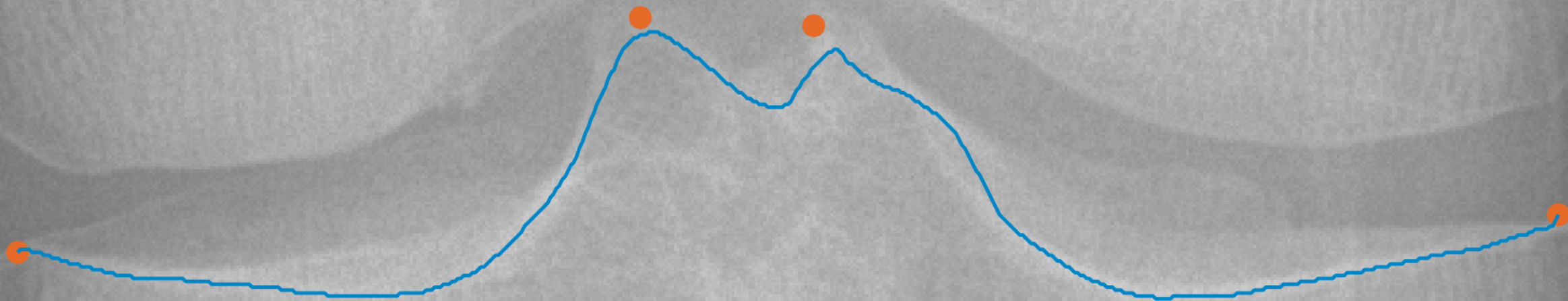
| | Baseline | | | 48 Month | | | p-values |
|-------------------------------------|-------------------------------|---------------------------------|----------------------------|-------------------------------|---------------------------------|----------------------------|-----------------|
| | Controls (k = 1419) | Progressors (k = 228) | Total (k = 1647) | Controls (k = 1419) | Progressors (k = 228) | Total (k = 1647) | |
| Age (years) | 62.7 ± 9.0 | 62.7 ± 8.2 | 62.7 ± 8.9 | 66.7 ± 9.0 | 66.7 ± 8.2 | 66.7 ± 8.9 | 0.995 |
| BMI (Kg/m²) | 29.3 ± 4.6 | 30.4 ± 4.6 | 29.5 ± 4.6 | 29.3 ± 4.8 | 30.7 ± 4.9 | 29.5 ± 4.8 | 0.002 |
| Gender (no. knees) | | | | | | | < 0.001 |
| F | 838 | 108 | 946 | - | - | - | |
| M | 581 | 120 | 701 | - | - | - | |
| Medial JSN grade (no. Knees) | | | | | | | < 0.001 |
| 0 | 620 | 31 | 651 | 620 | 0 | 620 | |
| 1 | 496 | 90 | 586 | 496 | 16 | 512 | |
| 2 | 303 | 107 | 410 | 303 | 128 | 431 | |
| 3 | 0 | 0 | 0 | 0 | 84 | 84 | |
| Center (no. Knees) | | | | | | | 0.583 |
| A | 319 | 41 | 360 | - | - | - | |
| C | 580 | 92 | 672 | - | - | - | |
| D | 468 | 84 | 552 | - | - | - | |
| E | 52 | 11 | 63 | - | - | - | |

k: the number of knees

"-" means no changes compared to baseline



* Excluding radiographs with materials, poor positioning or acquisition artifacts



WhE

| | | | | | | |
|-------|-------|-------|-------|-------|-------|-------|
| 5E-01 | 5E-01 | 8E-01 | 6E-01 | 7E-01 | 5E-01 | 9E-01 |
| | 9E-01 | 7E-01 | 7E-01 | 9E-01 | 9E-01 | |
| 0° | | 1E+00 | 9E-01 | 1E+00 | | |
| | Med | | | | Lat | |
| | | | 8E-01 | | | |

FSA

| | | | | | | |
|-------|-------|-------|-------|-------|-------|-------|
| 1E-04 | 2E-01 | 7E-01 | 4E-01 | 7E-01 | 5E-01 | 6E-02 |
| | 4E-02 | 4E-01 | 8E-01 | 1E-01 | 3E-01 | |
| 0° | | 6E-01 | 8E-01 | 8E-01 | | |
| | Med | | | | Lat | |
| | | | 7E-01 | | | |

Var

| | | | | | | |
|-------|-------|-------|-------|-------|-------|-------|
| 7E-01 | 7E-01 | 4E-01 | 7E-01 | 7E-01 | 8E-01 | 3E-01 |
| | 5E-01 | 3E-01 | 5E-01 | 3E-01 | 5E-01 | |
| 0° | | 4E-01 | 5E-01 | 5E-01 | | |
| | Med | | | | Lat | |
| | | | 7E-01 | | | |

| | | | | | | |
|-------|-------|-------|-------|-------|-------|-------|
| 9E-06 | 3E-04 | 5E-03 | 9E-03 | 2E-02 | 2E-02 | 3E-02 |
| | 2E-03 | 3E-02 | 4E-02 | 1E-01 | 2E-01 | |
| 90° | | 4E-02 | 6E-02 | 8E-02 | | |
| | Med | | | | Lat | |
| | | | 5E-01 | | | |

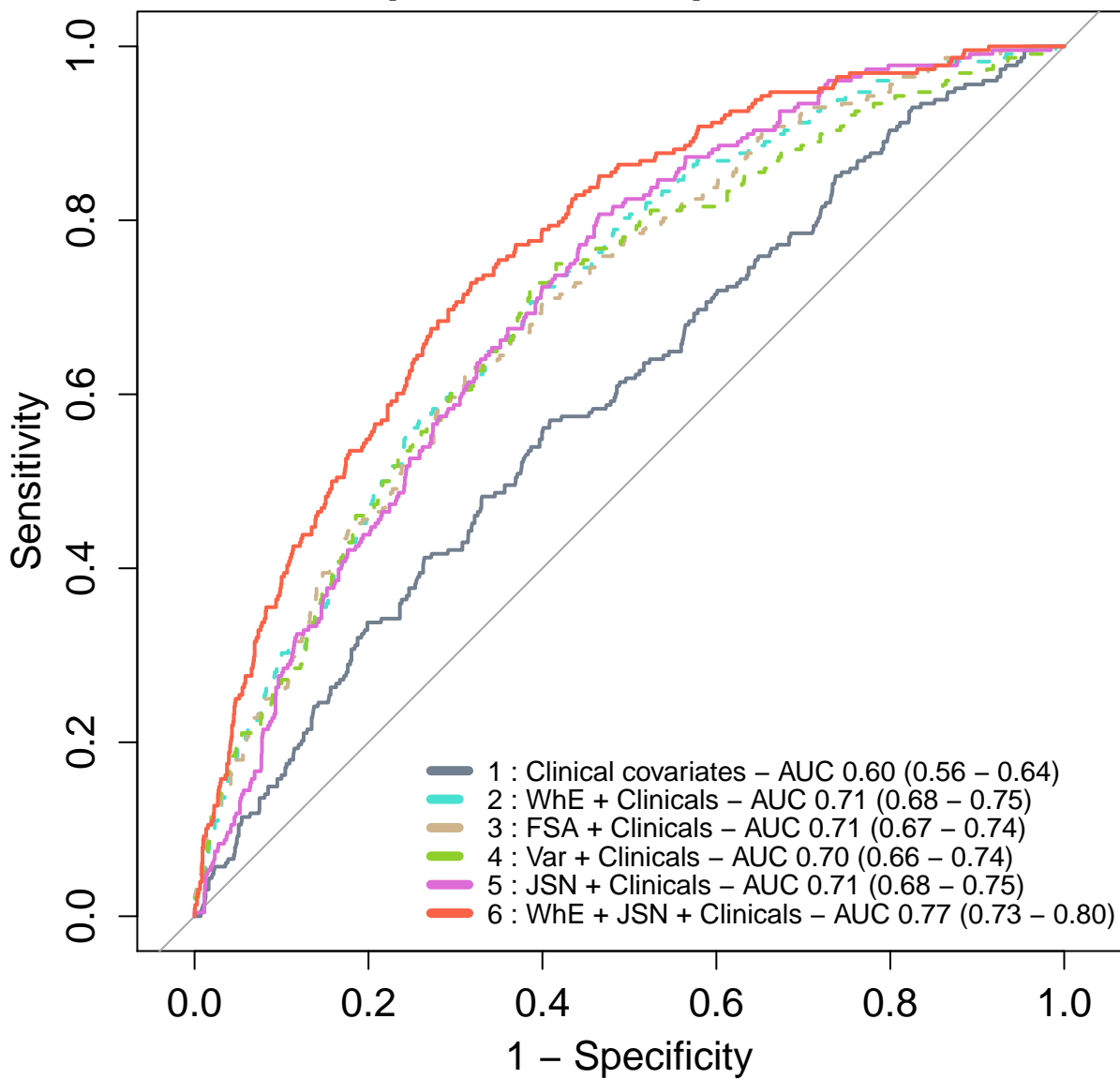
| | | | | | | |
|-------|-------|-------|-------|-------|-------|-------|
| 2E-01 | 1E-01 | 3E-01 | 3E-02 | 9E-02 | 6E-02 | 4E-02 |
| | 1E-02 | 6E-02 | 8E-02 | 2E-01 | 5E-01 | |
| 90° | | 3E-02 | 3E-03 | 1E-01 | | |
| | Med | | | | Lat | |
| | | | 5E-02 | | | |

| | | | | | | |
|-------|-------|-------|-------|-------|-------|-------|
| 7E-05 | 8E-03 | 4E-02 | 3E-02 | 4E-02 | 5E-02 | 5E-02 |
| | 7E-03 | 3E-02 | 1E-01 | 2E-01 | 2E-01 | |
| 90° | | 1E-01 | 6E-02 | 1E-01 | | |
| | Med | | | | Lat | |
| | | | 2E-01 | | | |

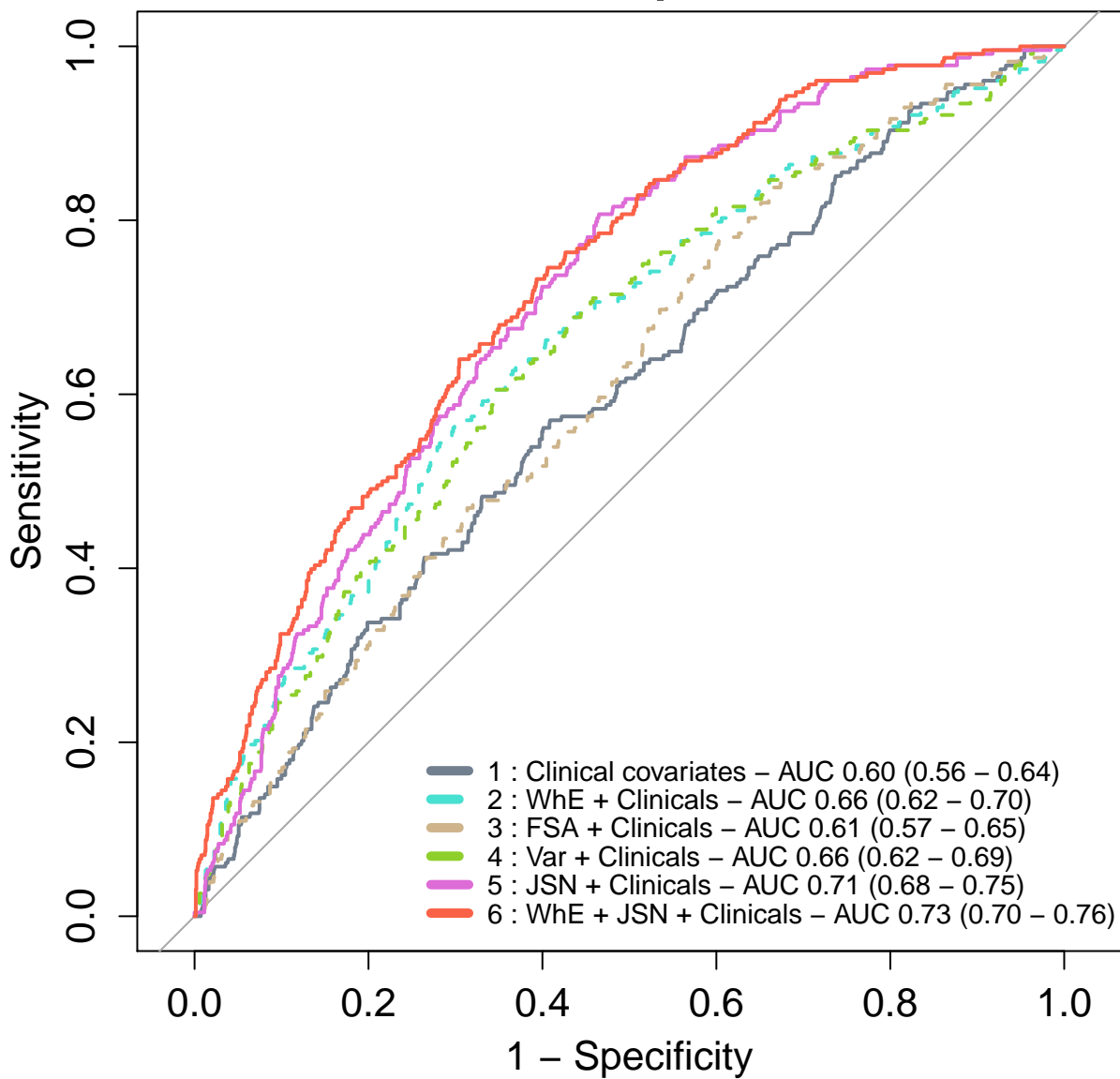
| | | | | | | |
|-------|-------|-------|-------|-------|-------|-------|
| 3E-02 | 7E-02 | 3E-01 | 2E-01 | 1E-01 | 1E-01 | 6E-01 |
| | 2E-01 | 4E-01 | 4E-01 | 6E-01 | 5E-01 | |
| 360° | | 5E-01 | 3E-01 | 5E-01 | | |
| | Med | | | | Lat | |
| | | | 5E-01 | | | |

| | | | | | | |
|-------|-------|-------|-------|-------|-------|-------|
| 8E-03 | 2E-01 | 5E-01 | 1E-01 | 2E-01 | 5E-01 | 5E-01 |
| | 1E-02 | 7E-01 | 5E-01 | 2E-01 | 9E-01 | |
| 360° | | 4E-01 | 1E-01 | 4E-01 | | |
| | Med | | | | Lat | |
| | | | 2E-01 | | | |

| | | | | | | |
|-------|-------|-------|-------|-------|-------|-------|
| 1E-01 | 2E-01 | 7E-01 | 4E-01 | 4E-01 | 4E-01 | 9E-01 |
| | 5E-01 | 8E-01 | 8E-01 | 9E-01 | 9E-01 | |
| 360° | | 8E-01 | 6E-01 | 8E-01 | | |
| | Med | | | | Lat | |
| | | | 7E-01 | | | |

Complete models performance

MANUSCRIPT

Partial models performance

Optimized models performance

